arXiv:astro-ph/0503098v1 4 Mar 2005

Ages, metallicities and α-element enhancement for galaxies in Hickson compact groups

C. Mendes de Oliveira [1,2,3], P. Coelho [1,4], J.J. González [5] and B. Barbuy [1]

ABSTRACT

Central velocity dispersions and eight line-strength Lick indices have been determined from 1.3Å resolution long-slit spectra of 16 elliptical galaxies in Hickson compact groups. These data were used to determine galaxy properties (ages, metallicities and α-element enhancements) and allowed a comparison with the parameters determined for a sample of galaxies in lower density environments, studied by González (1993). The stellar population parameters were derived by comparison to single stellar population models of Thomas et al. (2003) and to a new set of SSP models for the indices Mg_2, Fe5270 and Fe5335 based on synthetic spetra. These models, based on an update version of the fitting functions presented in Barbuy et al. (2003), are fully described here. Our main results are: (1) the two samples have similar mean values for the metallicities and [α/Fe] ratios, (2) the majority of the galaxies in compact groups seem to be old (median age of 14 Gyr for eight galaxies for which ages could be derived), in agreement with recent work by Proctor et al. (2004). These findings support two possible scenarios: compact groups are either young systems whose members have recently assembled and had not enough time to experience any merging yet or, instead, they are old systems that have avoided merging since their time of formation.

Subject headings: galaxies: kinematics — galaxies: stellar populations — galaxies: elliptical and lenticular — galaxies: interactions — galaxies: formation —

[1]Universidade de São Paulo, IAG, Departamento de Astronomia, Rua do Matão 1226, Cidade Universitária, 05508-900, São Paulo, SP, Brazil, oliveira@astro.iag.usp.br, pcoelho@usp.br, barbuy@astro.iag.usp.br

[2]Max-Planck-Institut für Extraterrestrische Physik, Giessenbachstrasse, D-85748 Garching b. München, Germany, oliveira@mpe.mpg.de

[3]Universitäts-Sternwarte der Ludwig-Maximilians-Universität, Scheinerstrasse 1, D-81679 München, Germany, oliveira@usm.uni-muenchen.de

[4]Max-Planck-Institut für Astrophysik, Karl-Schwarzschild-Str. 1, D-85741 Garching b. München, Germany, pcoelho@mpa-garching.mpg.de

[5]Instituto de Astronomia, UNAM, Apdo Postal 70-726, 04510 Mexico D.F., Mexico

1. Introduction

The conventional scenario for the evolution of compact groups, supported by n–body simulations, is that their members will interact and merge into one single elliptical galaxy, if they are genuine high-density systems. Compact groups are, therefore, ideal environments in which to study the formation of elliptical galaxies through mergers and the effects of collisions on galactic evolution although this requires that the lifetime of the group be longer than the merging timescales between member galaxies. We currently lack important information on how long the member galaxies of a compact group have been together as a compact entity although we have qualitative information that some dynamical interaction among the galaxies has happened in the majority of the groups.

While there is plenty of evidence that the rate of *interactions* (which leave the two galaxies distinct) is high among compact group galaxies, studies of optical colors and galaxy morphologies suggest that the rate of ongoing mergers is low. However, it may be more difficult to recognize merger remnants in compact groups than in other environments, since the forces exerted by the member group galaxies tend to disrupt long tails and extensions created in galactic collisions (Barnes & Hernquist 1992). In addition, mergers in compact groups may be different in nature if the colliding galaxies have a smaller reservoir of gas. This may actually be the case since it has been shown that at least cold gas seems to be depleted from small galaxy groups, possibly due to interactions.

Several programs have been initiated to develop more sensitive tests of merging history in elliptical galaxies in compact groups. In this context, a comparison of the stellar populations of elliptical galaxies in compact groups with those of galaxies in other environments are of great interest and may provide a quantitative measure of the effects of mergers.

A number of papers have studied the stellar populations of early-type galaxies in clusters and in lower density environments (e.g. Rose et al. 2004; Jorgensen 1997; Bernardi et al. 1998; Proctor et al. 2004). In compact groups, however, there are very few previous studies. Proctor et al. (2004) derived ages, metallicities and α-enhancements of stellar populations for a sample of 17 elliptical galaxies and 9 spiral bulges in compact groups and found that the HCG galaxies are generally older and more metal rich than their field counterparts. Although Jorgensen (1997) argues that it is not possible to derive unique galaxy parameters from the observables, some more recent studies, e.g. Thomas et al. (2003, hereafter TMB03), have developed stellar population models that include element abundance ratio effects and which can provide a derivation of age, total metallicity and element ratios from Lick absorption line indices. A complication is however the degeneracy between age and horizontal branch morphology, which comes from the fact that the presence of warm horizontal branch stars may strengthen the Balmer absorption lines, possibly mimicing a younger stellar population age (e.g. Maraston & Thomas 2000). This problem still remains to be solved.

The main contribution of this paper is the determination of internal velocity dispersions and eight Lick/IDS indices for 16 galaxies in HCGs (three of which are in common with the sample of Proctor et al. 2004). Our new measurements were compared with models from TMB03, and with a

new set of SSP models, presented here for the first time, to derive ages, metallicities and α-element enhancements for the galaxies.

This paper is organized as follows. Section 2 describes our observations and reductions. In Section 3 results from the comparisons between the HCG and control sample regarding their ages, metallicities, and α enhancements are shown. In addition, fitting functions for the indices Mg_2, Fe5270 and Fe5335 based on synthetic spectra (Barbuy et al. 2003), and a new set of SSP model indices are presented. In Section 4 we discuss the possible selection effects affecting our sample, the main contributions given by other work in the literature and the insights provided by our new data regarding the merging histories of the compact group galaxies.

2. Observations and Reductions

We observed 16 of the 28 Hickson compact group (Hickson 1982) elliptical galaxies south of declination –10°, between R.A's 19^h and 03°, and brighter than $B_T = 16$ mag.

Long-slit spectra for the galaxies were taken at the Anglo Australian Observatory with a 25cm camera, a 1200 V grating and a TEK CCD on the AAT 3.5m telescope. These spectra cover the range $\lambda\lambda \sim 4810 - 5630$ Å with 1.34 Å resolution FWHM. The wavelength and spatial scale were ~ 0.79 Å/pixel and 1.03 arcsec/pixel respectively. Each galaxy was observed twice along its major axis. The total exposure times ranged from 800s to 2000s. A slit width of 1.5 arcsec was used.

Radial velocities, internal velocity dispersions and the Lick/IDS indices Hβ, Mg_1, Mg_2, Mg_b, Fe5015, Fe5270, Fe5335, Fe5406, inside an aperture of radius $r_{eff}/2$ (where r_{eff} is the effective radius of the galaxy, obtained from the fit to a de Vaucoleurs profile, de Vaucoleurs 1948) were obtained using the technique developed by González (1993). In this method the spectra of each galaxy and template are compared in Fourier space. Optimal templates were constructed from an optimal linear combination of stellar spectra of late-type dwarf and giant stars obtained in the same nights when the galaxy observations were made (see González 1993, at http://www.astroscu.unam.mx/∼jesus/, for the reduction procedure details). Line-strength measurements were made in the Lick/IDS system as introduced by Burstein et al. (1984) and refined by Worthey et al. (1994). The transformation to the Lick/IDS system was done by using stars from Faber et al. (1985)'s list observed during our run.

We used a control sample taken from the list of galaxies in loose groups and in the field studied by González (1993, hereafter the "field" sample), observed at Lick Observatory with the 120-inch Shane Telescope, at a resolution of FWHM = 2.7 – 3.3 Å. Velocity dispersions and line-strength indices for the galaxies in the control sample were derived in the same manner as for the galaxies in the compact group sample. For comparison, two of the elliptical galaxies in the control sample were observed in the run when the spectra for the compact-group galaxies were obtained. Their derived velocity dispersion and line-strength indices are in excellent agreement (within the quoted errors of 5%) with those obtained independently by González (1993).

All spectra were extracted inside a radius of $r_{eff}/2$ in order to sample similar parts of the galaxies, and avoiding the need of using uncertain aperture corrections. This is important in our case since the control sample is composed of galaxies which are quite nearby, with a median radial velocity of 2300 km s^{-1}, while the sample of compact group galaxies has a median velocity of 7200 km s^{-1}.

3. Results

The kinematic data for the Hickson compact group galaxies are presented in Table 1. Radial velocities and velocity dispersions were derived within an aperture of radius $r_{eff}/2$. The effective radii and values for the surface brightness measured within the effective radii, listed in columns 2 and 3 were taken from Zepf and Whitmore (1993) for the galaxies in common and were derived from B images taken at CFHT (Mendes de Oliveira 1992), for the remaining galaxies. In the fourth column, the S/N of the spectra are listed. These were obtained within the spectral window 4900 to 5500 Å, derived similarly to those obtained by González (1993) for the control sample. The Lick indices and their estimated errors, measured within an aperture of radius $r_{eff}/2$, are presented in Table 2. The galaxies marked with an asterisk are known to have emission lines, and for these the values measured for the Hβ indices are very uncertain, and therefore not given.

3.1. Emission lines

Fig. 1 shows four of the five examples of emission-line elliptical galaxies found in our sample. In each panel we show, at the top, the wavelength calibrated spectrum, in the middle, a template spectrum obtained by summing several stellar spectra and, at the bottom, the subtraction of the two upper spectra, clearly showing the emission lines Hβ at 4861 Å and [OIII] at 5007 Å.

Emission lines were visible in five of the 16 elliptical galaxies in our sample. This may be compared to the study of 12 HCG elliptical galaxies by Rubin, Hunter and Ford (1991). They found that emission lines were present in 10 of those galaxies. It is tempting to compare the frequency of emission lines found in these studies with that of Phillips et al. (1986), who find a 60% incidence of emission lines in early-type galaxies in loose groups. However, a meaningful comparison cannot be made between these results as the detection of faint emission lines depends strongly on the resolution and S/N ratio of the spectrum. For the same reason, our results are not inconsistent with those of Rubin et al. (1991) since their spectra were centered near 6500 Å allowing them to detect Hα, [NII], and S[II] emission lines.

Emission lines were visible in 12 of the 28 (43%) elliptical galaxies from González' sample. This fraction is similar to what we find for the compact groups (5 in 16, 31%) although the average S/N for the González' sample is almost an order of magnitude higher than ours. The numbers of galaxies in the samples are still very small and the data quality too inhomogeneous for a meaningful

comparison of the frequency of emission line elliptical galaxies in different environments.

3.2. Mg_b, Fe5270 and Fe5335 indices

We plot in Fig. 2 the Mg_b and the $< Fe >$ Lick/IDS indices against velocity dispersion, for all galaxies in our sample and in the control sample. In Fig. 3 is plotted the non-standard Lick/IDS index defined by González (1993), [MgFe], as a function of velocity dispersion. These plots show that the HCG elliptical galaxies have the same mean Mg_b and $< Fe >$ line strengths as do galaxies in the control sample. In both samples, the typical values indicate an excess of Mg absorption with respect to the metallicity relation defined by the galactic globulars. This can be clearly seen in Fig. 4. This figure shows a plot of Mg_b against $< Fe >$ line strengths for the compact group and the control samples. The continuous line is the locus of the galactic globular clusters. The point at the bottom left of the diagram is the galaxy HCG 04d.

Two other studies have measured Mg and Fe line-strength indices for galaxies in our compact group sample. Galaxies N7176 (or 90b) and N7173 (or 90c) were measured by Burstein et al. (1987) and galaxies 14b, 86a and 86b were measured by Proctor et al. (2004). A comparison between our measurements and those other measurements, after employing aperture corrections (Jorgensen et al. 1995) to transform all indices to a common radius, are in agreement within 30%, or better.

3.3. Simple stellar populations models with variable $[\alpha/Fe]$

In normal luminous elliptical galaxies, the Mg excess has been interpreted as an indication of a higher than solar [Mg/Fe] abundance ratio, probably due to the dominant SNII over SNIa enrichment in these galaxies (González 1993; Worthey, Faber and González 1992). From the large dataset of nuclear line strengths of the Lick group, presented in Trager et al. (1998), it is shown that low velocity dispersion objects exhibit solar [Mg/Fe] and more massive systems are overabundant in magnesium. Luminous HCG elliptical galaxies are not different in this respect.

Therefore, for the study of stellar populations in ellipticals it is crucial to employ population models that take into account α-element enhancements. Very few models that allow derivation of both [Z/H] and [α/Fe], or alternatively [Fe/H] and [α/Fe], are available.

TMB03 present Simple Stellar Population (SSP) models based on the population synthesis code presented in Maraston (1998, 2005), in which the fuel consumption theorem (Renzini & Buzzoni 1986) is employed. The models account for the α-enhancement by using synthetic spectra calculations by Tripicco & Bell (1995, hereafter TB95), and provide Lick indices for SSPs covering ages from 1 to 15 Gyr, metallicities from 1/200 to 3.5 solar and variable element abundance ratios.

As an alternative approach, we computed a set of SSP models based on synthetic stellar spectra as described in Barbuy et al. (2003). The computed grid of synthetic spectra covers the range 4600-

5600 Å for stellar parameters 4000 $\leq$ T_{eff} $\leq$ 7000 K, 5.0 $\leq$ log g $\leq$ 0.0, -3.0 $\leq$ [Fe/H] $\leq$ 0.3, and two values of chemical mixture [α/Fe] = 0.0 and +0.4 dex (the α-elements considered are O, Mg, Si, S, Ar, Ca, Ne, Ti). In the present work, a new set of spectra with [α/Fe] = +0.2 was computed, in order to better take into account the dependence of the indices on the α-enhancements [α/Fe].

The indices Mg_2, Fe5270 and Fe5335 were measured for the whole parameter range and fitting functions of the form below (where $\theta = 5040/T_{eff}$) were derived through a Levenberg-Marquadt algorithm

index = exp $[(a + b(log\theta) + c(log\theta)^2 + d(log\theta)^3 + e(logg) + f(logg)^2 + g(logg)^3 + h([Fe/H]) + i([Fe/H]^2) + j([Fe/H]^3) + k([\alpha/Fe]) + l(log\theta)(logg) + m(log\theta)([Fe/H]) + n(log\theta)([\alpha/Fe]) + o(log\theta)^2(logg) + p(log\theta)(logg)^2)]$

The new coefficients, which supersede the ones presented in Barbuy et al. (2003), are presented in Tables 3, 4 and 5. The zero-point constants to calibrate the fitting functions to the Lick/IDS system were obtained following the procedure described in detail in Barbuy et al. (2003, Section 3.1). Shortly, synthetic indices are computed with the fitting functions for the standard Lick/IDS stars presented in Worthey et al. (1994). The input parameters for the fitting funcions T_{eff}, log g and [Fe/H] are obtained directly from the catalog in Worthey et al. (1994). The value of [α/Fe] is adopted for each star as a function of [Fe/H], given the $[Fe/H]$ vs. $[\alpha/Fe]$ relation presented in McWilliam (1997). The synthetic indices computed are then compared with the measured indices in the Lick/IDS system and a calibration constant can be obtained by least-square fitting. The calibration constants are presented in Table 6.

Indices for SSPs were then derived by combining these fitting functions with isochrones of Demarque et al. (2004). The isochrones of Demarque et al. (2004) were preferred over other α-enhanced isochrones available in the literature (Salasnich et al. 2000, Straniero et al. 1992, Salaris, Chieffi & Straniero 1993, Salaris & Weiss 1998) because their chemical mixture for the α-enhancements are closer to the mixture adopted in Barbuy et al. (2003) for the synthetic stellar grid. Along the isochrone synthesis procedure, the indices were weigthed by the visual absolute magnitude (Greggio 1997). The models were computed for a limited range of ages (4 $\leq$ t $\leq$ 16 Gyr) and metallicities (0.008 $\leq$ Z $\leq$ 0.04), suitable to the present analysis of the HCG galaxies. For this high metallicity range, a strong contribution from blue horizontal branch stars, not taken into account in our models, is not expected.

One caveat to consider is that the fitting functions presented here, and employed in the SSP models, are strictly valid down to effective temperatures equal to 4000K, which is the lower limit of the temperature range of the synthetic grid in Barbuy et al. (2003). In cases where the isochrones require lower temperature stars, the fitting functions were extrapolated. A few stellar spectra for giants with temperatures of 3800K were computed, employing Plez et al. (1992) model atmospheres. It was verified that the extrapolated stellar indices differ from the measured ones typically by amounts of the order of the uncertainties on the fitting functions (last line of Tables 3-5), and therefore the error introduced in the integrated indices due to the extrapolation are smaller than

10%. A further investigation of the behavior of these indices in K and M stars will be discussed elsewhere. In particular, it is shown in Coelho et al. (2005, in preparation) that TiO bands become strong in metal-rich very cool stars, blending the Mg_2 feature, essentially preventing the use of this index at very low stellar temperatures.

The SSP model indices for Mg_2, Fe5270 and Fe5335 are given in Appendix A.

As explained in detail in TMB03, their fitting functions are those by Worthey et al. (1994), and corrections to account for the [α/Fe] enhancements were based on calculations of synthetic spectra by TB95 (through the so-called response functions), following an extension of the method proposed by Trager et al. (1998). The use of the fitting functions that are explicitly dependent on the [α/Fe] parameter is an alternative approach to employing empirical fitting functions corrected by response functions (TMB03). The former are based on spectra that have all the α-elements enhanced together, while the latter incorporates changes in the indices due to individual element variations. It is not clear if the effect of the enhancement of all α-elements together is a linear combination of the effects due to individual abundance variations. This question arises because an important effect related to the α-elements is that they are electron donors. The continuum in G-M stars forms mainly by free-free and bound-free transitions of H^-, whereas the amount of H^- present in their atmospheres depends on the electrons captured by Hydrogen atoms which come from the α-elements in particular (Fe is also an important electron donor). Therefore, an overall enhancement of the α-element abundance can have an impact in the continuum (and therefore in the indices) that is different from combining the impact of varying the abundance of each element individually through response functions.

3.4. Stellar Populations of the HCG galaxies

The indices measured from the spectra of sample galaxies were compared to the SSP models, and the luminosity weighted average ages t, metallicities [Z/H] and α-enhancements [α/Fe] were derived.

A fortran code (kindly provided to us by D. Thomas) inspects correlations between Hβ and the metallic indices to find the best fit (t, [Z/H], [α/Fe]) for each galaxy.

Only measurements with the smallest errors, i.e. Hβ errors less than 0.25 and fractional uncertainties for both Mg and Fe indices lower than 10%, were used in the derivation of the galaxy parameters. Given the ages derived with the TMB03 models, values for [Fe/H], [Z/H] and [α/Fe] were also derived using the SSP models calculated in this work, by selecting the best model through a χ-square criteria weighted by the measurements errors. The age estimations were based entirely on TMB03 models since they carried out extensive comparisons and corrections relative to observed models, which is needed for the use of computed Hydrogen lines, and indices such as Hβ. These derived stellar population parameters are presented in Table 7 and the typical estimated errors of the parameters are 2 Gyr for age and +0.2 dex for [Z/H] and [α/Fe]. The parameters derived with

TMB03 models are shown in columns 2 - 4 of Table 7 and those derived using our models are shown in columns 5 - 7 of the same table. For the galaxies with emission and/or those whose errors on Hβ were too large (three galaxies), no age determination was attempted.

The problem of corrections of the galactic abundance pattern, as pointed out by Proctor et al. (2004) in the use of SSP models by Vazdekis (1999), is not an issue in our case when the SSP models computed here are employed, because this correction should be applied only to models that were built based on observed stars. In addition, Thomas et al. (2005) concluded that corrections for the local abundance pattern has no significant impact on their SSP models, when [α/Fe] is solar/supersolar.

There is a trend in the sense that the [α/Fe] obtained by the models calculated in this work are higher than those by TMB03 by ≈ 0.1 dex, and a comparison of the two sets of models employed can be seen in Fig. 5. Nevertheless, given the completely different ingredients of the two sets of models (fitting functions, isochrones and SSP synthesis prescriptions), the agreement is remarkable.

In Figs. 6 and 7 we plot the values for the HCG galaxies, the SSP models from TMB03 and the corresponding values for the field galaxies from González (1993) in the [MgFe]' vs. Hβ and Mg$_b$ vs. $< Fe >$ diagrams respectively.

Though the statistics of the compact group galaxies is still small, it is possible to see that the locus of the compact group galaxies is characterized by old ages, solar and super-solar metallicities and α-enhancement. As a comparison, the field galaxies from the sample of González seem to span a wider parameter range. However, these also span a wider range of velocity dispersions (including less massive galaxies), as can be seen in Figs. 2 and 3.

4. Discussion

4.1. Possible selection effects

One point that should be kept in mind is that the sample of HCGs selected by Hickson (1982) is biased towards high surface brightness *groups*. At first sight, this may appear to preferentially select the highest surface brightness galaxies, which, in turn, could be biasing our results (to obtain preferentially old ages).

In order to test this we have made a comparison of the surface brightnesses within r$_{eff}$ of the galaxies in the control sample and in the HCG sample. We found that the two distributions can be driven from the same parent population with a confidence level of 95% (using the KS test), showing that we are comparing galaxies of similar surface brightnesses, in the HCG and control samples.

Another point that could be thought to bias our sample is the fact that we discard galaxies which have emission lines when computing ages for the objects. This may select against galaxies which have suffered minor accretion events, although it is unlikely that we have missed major

mergers (which would be recognized also from their other optical properties). This is not a problem in Proctor et al's (2004) study, since they do not perform such emission-line selection (because they use 20 different Lick indices for determination of the galaxy parameters). The determination of old ages for compact group galaxies seems, therefore, to be quite a robust result and not a selection effect.

4.2. Possible Outliers

The two best candidate elliptical galaxies with young stellar populations and/or mergers in our HCG sample are 04d and 14b, which are the galaxies with the lowest velocity dispersions and lowest values of Mg_b. Note that in Figs. 2, 3 and 4, galaxies 04d, 14b are in all cases below the line followed by the control sample galaxies. Galaxy 04d was studied in detail by Zepf et al. (1991). Its surface brightness profile is well fit by an $r^{1/4}$-law profile and it seems to be a genuine low-mass elliptical galaxy (Zepf et al. 1991). HCG 04d is one of the bluest elliptical galaxies in Hickson's catalogue and it is significantly bluer than galaxies of similar mass in other environments. Galaxy HCG 14b was one of the few outliers in the diagram $M_8 \times r_{eff}$ shown by Mendes de Oliveira (1992), where M_8 is the absolute magnitude within an aperture of radius equals to 8 h^{-1} kpc, suggesting that this galaxy has a very extended profile for its luminosity, resembling a cD galaxy in this aspect. This can be confirmed by the large measurement of its effective radius. However, Proctor et al. (2004) classify this galaxy as a spiral bulge.

4.3. Other important work from the literature

The α-enhancement in galaxies, first pointed out by Peletier (1989) and Worthey et al. (1992), was reviewed by Worthey (1998), Peletier (1999) and Jorgensen (1999), from the observed Mg_2 vs. Fe indices. Trager et al. (1998), TMB03, and the present work derive more quantitatively the α-enhancements based on calculations of synthetic spectra. The present sample galaxies also show overabundance in magnesium-to-iron.

Several studies have tried to tackle the problem of environmental effects on the spectral properties of elliptical galaxies. Rose et al. (1994) found that ellipticals/S0 in low density environments are considerably more metal-rich, a result confirmed by Proctor et al. (2004) and Thomas et al. (2005). In addition, galaxies in the field have been found to be younger than cluster counterparts (Bernardi et al. 1998; Proctor et al. 2004; Thomas et al. 2005). However, Proctor et al. (2004) found that HCG galaxies are older than field galaxies and are more consistent with the mean age of cluster galaxies. In fact, our result goes in the same direction: we find that the HCG galaxies are generally older than their counterparts in looser environments.

The fraction of possible ongoing mergers in compact groups has been determined through methods other than by studying the stellar populations of the elliptical galaxies, as we are doing

here. The optical colors of a sample of early-type galaxies and their infrared properties were studied by Zepf et al. (1991) and Moles et al. (1994). They found the merging rate to be between 5 and 12%. However, the candidate mergers they present are most probably early-type galaxies with small contribution of a young stellar component, instead of major mergers. Our determinations of ages, metallicities and α-element abundances for compact group galaxies also point to a low fraction of mergers in compact groups. These results have important bearings on the age of the group, which is discussed in the following.

4.4. Implications of the results

Our result as well as Proctor et al.'s (2004) main result that HCG galaxies are generally old contradicts the expectations from most formation scenarios for compact groups. Diaferio et al. (1994) proposed that loose groups may be continuously collapsing to form compact groups, predicting that about 30% of the elliptical galaxies in compact groups should be mergers, which is not supported by the study of the stellar populations of the elliptical galaxies presented here and in Proctor et al. (2004). One other scenario, proposed by Governato et al. (1996), suggests that galaxies in compact groups merge to form a massive elliptical galaxy and by secondary infall of surrounding galaxies, the systems maintain their status as HCGs. According to this scenario, merging of at least one or two massive galaxies happened at redshifts between z=1 and 0.35, for their most probable realizations, which would also be in disagreement with our results. One scenario that would be in agreement with our observations is that based on simulations by Athanassoula et al. (1997), who suggest that if the dark matter is distributed in a common group halo, rather than individual galaxy halos, and assuming a high halo-to-total mass ratio and a density distribution with very little central concentration, merging is suppressed and HCGs would be dynamically very long-lived systems (i.e. they could live for more than a Hubble time). Although the assumption of a common massive halo around the group is supported by the observations, the lack of central concentration is not (e.g. Zabludoff and Mulchaey 1998). In fact, the opposite scenario is also supported by our findings, i.e. one in which Hickson compact groups are young systems where merging happens so fast (in a small fraction of the Hubble time) that few or no merged objects are seen while the group is still recognizable as a group.

One other important point to complement this discussion is that compact groups exhibit a fraction of early-type galaxies higher than that in the field or in loose groups (Hickson et al. 1988), and more similar to clusters. If galaxy-galaxy merging is not responsible for the high early-type fractions, as suggested from our results on the stellar populations, it is possible that the effects of the environment are relatively unimportant at the current epoch and that the similarity in the frequency of red galaxies and in the stellar populations of galaxies in rich clusters and Hickson compact groups reflects conditions at the time of galaxy formation.

5. Acknowledgments

We are very grateful to Daniel Thomas and Robert Proctor for making their codes available and for very helpful discussions. We would also like to thank Mike Bolte for useful comments on an early version of the manuscript and an anonymous referee for suggested changes which improved the paper. We thank Natarajan Visvanathan (in memoriam) for obtaining the data for this study. CMdO would like to acknowledge support from the Brazilian FAPESP (projeto temático 01/07342-7), PRONEX, the Alexander von Humboldt Foundation and the Max-Planck-Institut für Extraterrestrische Physik, where this work was completed. PC acknowledges a Fapesp PhD fellowship n° 2000/05237-9. We made use of the Hyperleda database and the NASA/IPAC Extragalactic Database (NED). The latter is operated by the Jet Propulsion Laboratory, California Institute of Technology, under contract with NASA.

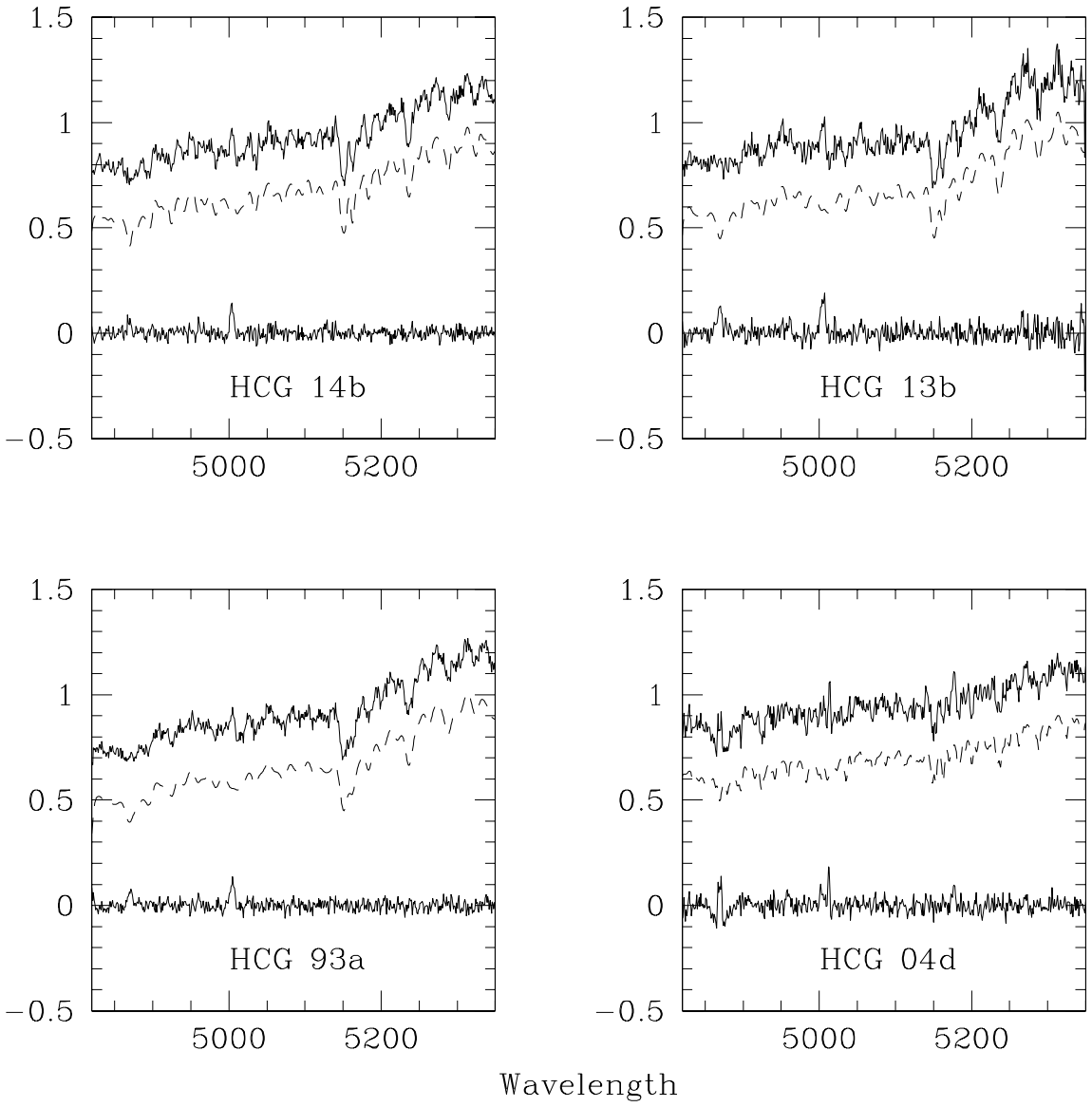

Fig. 1.— Spectra of four selected galaxies in our sample, which present emission lines. For each panel: top line – wavelength calibrated spectrum; middle (in broken lines) – optimal template; bottom line – difference between the spectrum and the template. In the latter one can easily see the lines in emission (Hβ at 4861 Å and [OIII] at 5007 Å) Five of the 16 elliptical galaxies in our sample showed emission lines in their spectra. The y axis is an arbitrary scale.

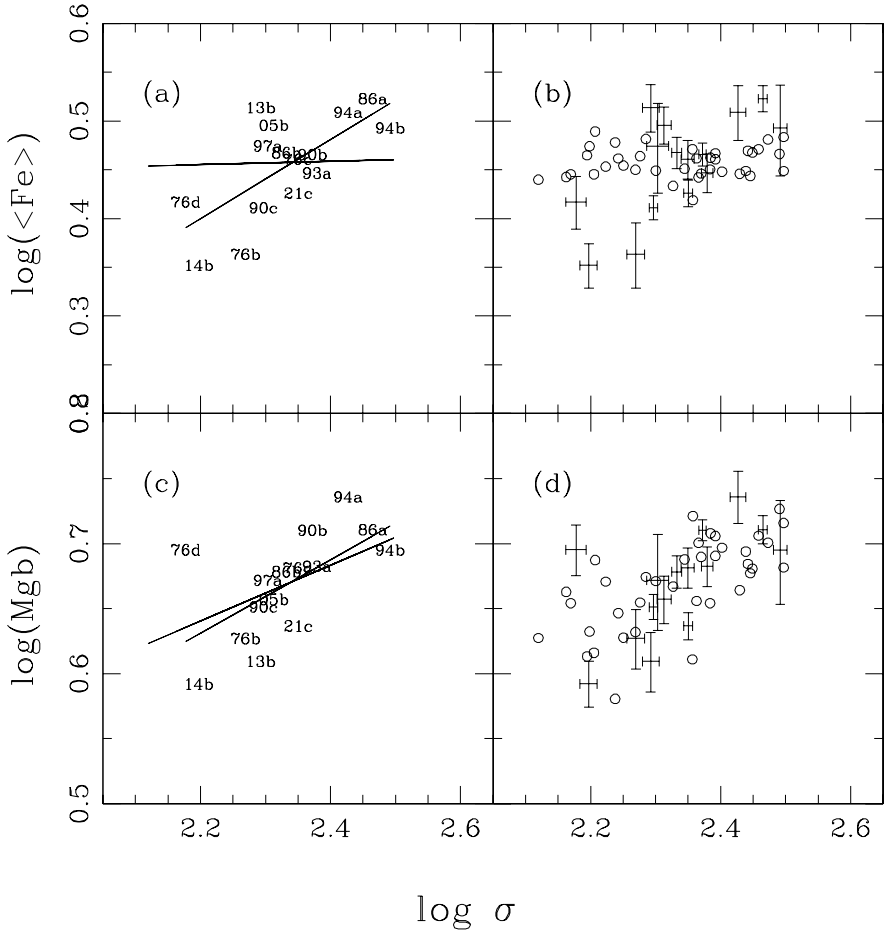

Fig. 2.— A plot of $< Fe >$ and Mg_b *vs.* velocity dispersion for 16 galaxies in compact groups (galaxy 04d is not plotted; its indices are out of the scale of the plot). Diagrams (a) and (c) identify the objects by their Hickson catalogue ID numbers. The straight lines are the mean relations for the compact group and the control samples. In diagrams (b) and (d) the open circles indicate the galaxies in the control sample and the center of the error bars indicate the galaxies in the compact groups.

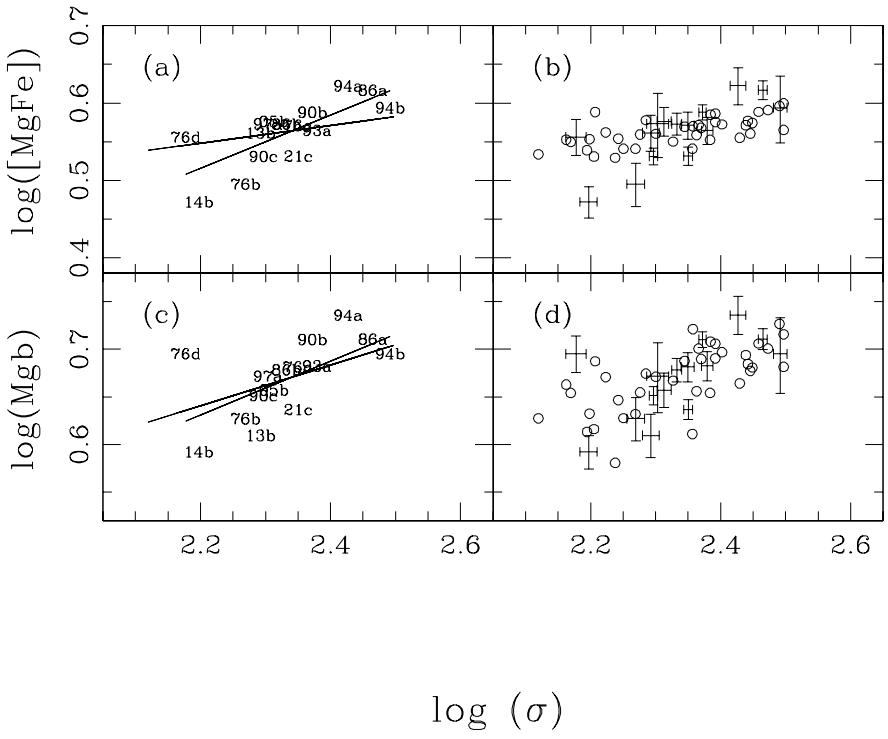

Fig. 3.— A plot of [MgFe] and Mg_b *vs.* velocity dispersion for 16 galaxies in compact groups (galaxy 04d is not plotted; its indices are out of the scale of the plot). The index [MgFe] is defined as [MgFe] = sqrt(Mg b . $< Fe >$) by González (1993). Diagrams (a) and (c) identify the objects by their Hickson catalogue ID numbers. The straight lines are the mean relations for the compact group and the control samples. In diagrams (b) and (d) the open circles indicate the galaxies in the control sample and the center of the error bars indicate the galaxies in the compact groups.

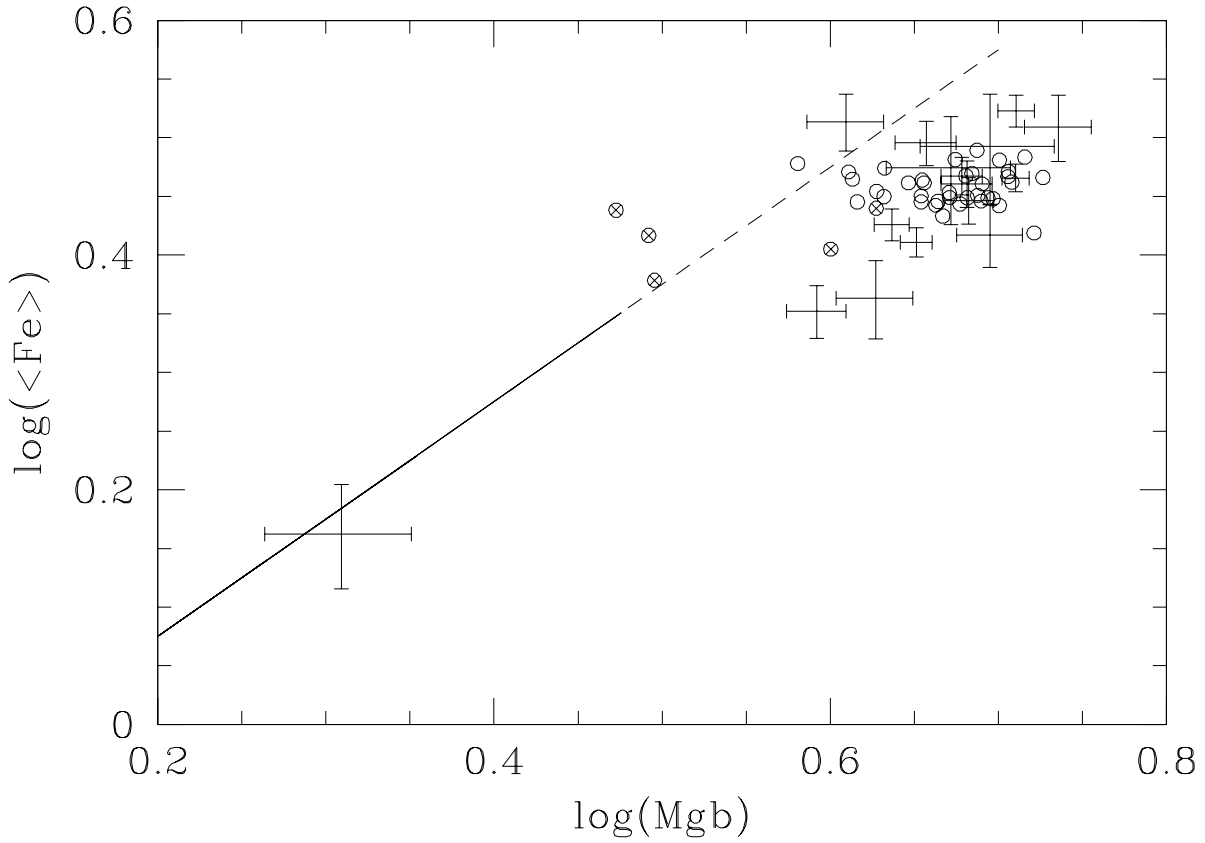

Fig. 4.— Plot of Mg_b against $< Fe >$ line strengths for the compact groups (indicated by the error bars) and the control sample (open circles). Four galaxies from the control sample with velocity dispersions smaller than 100 km/s are indicated as crossed circles (these are not included in the previous figures). The continuous line is the locus of the galactic globular clusters and the broken line is an extrapolation of it.

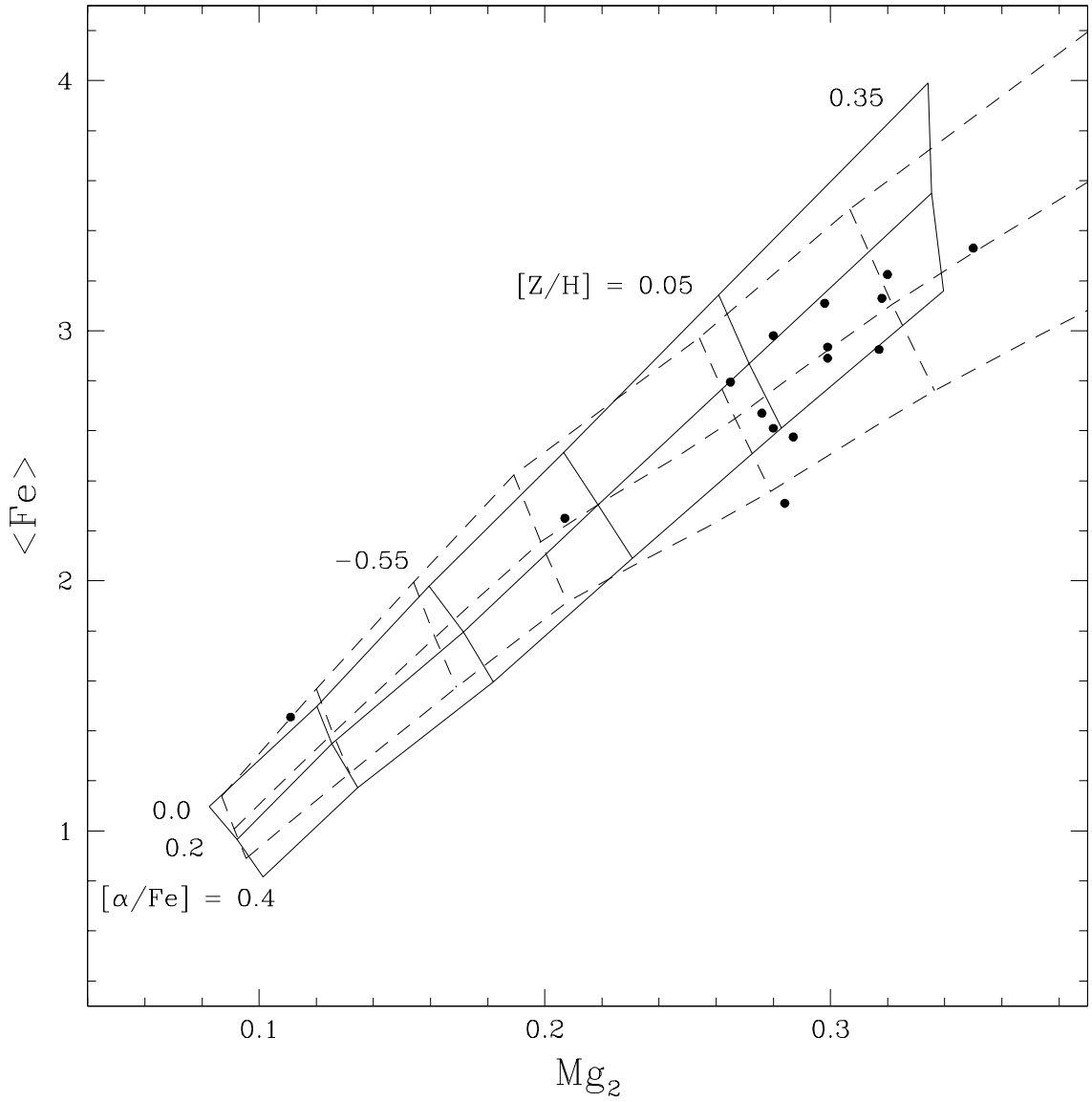

Fig. 5.— Compact group galaxies (filled circles) in a <Fe> vs. Mg_2 diagram, overplotted with two sets of SSP models, where the TMB03 models are the dashed lines, and models computed in this work are the solid lines. Labels are given to illustrate the loci occupied by different stellar population parameters. The models are plotted for an age t = 12 Gyr.

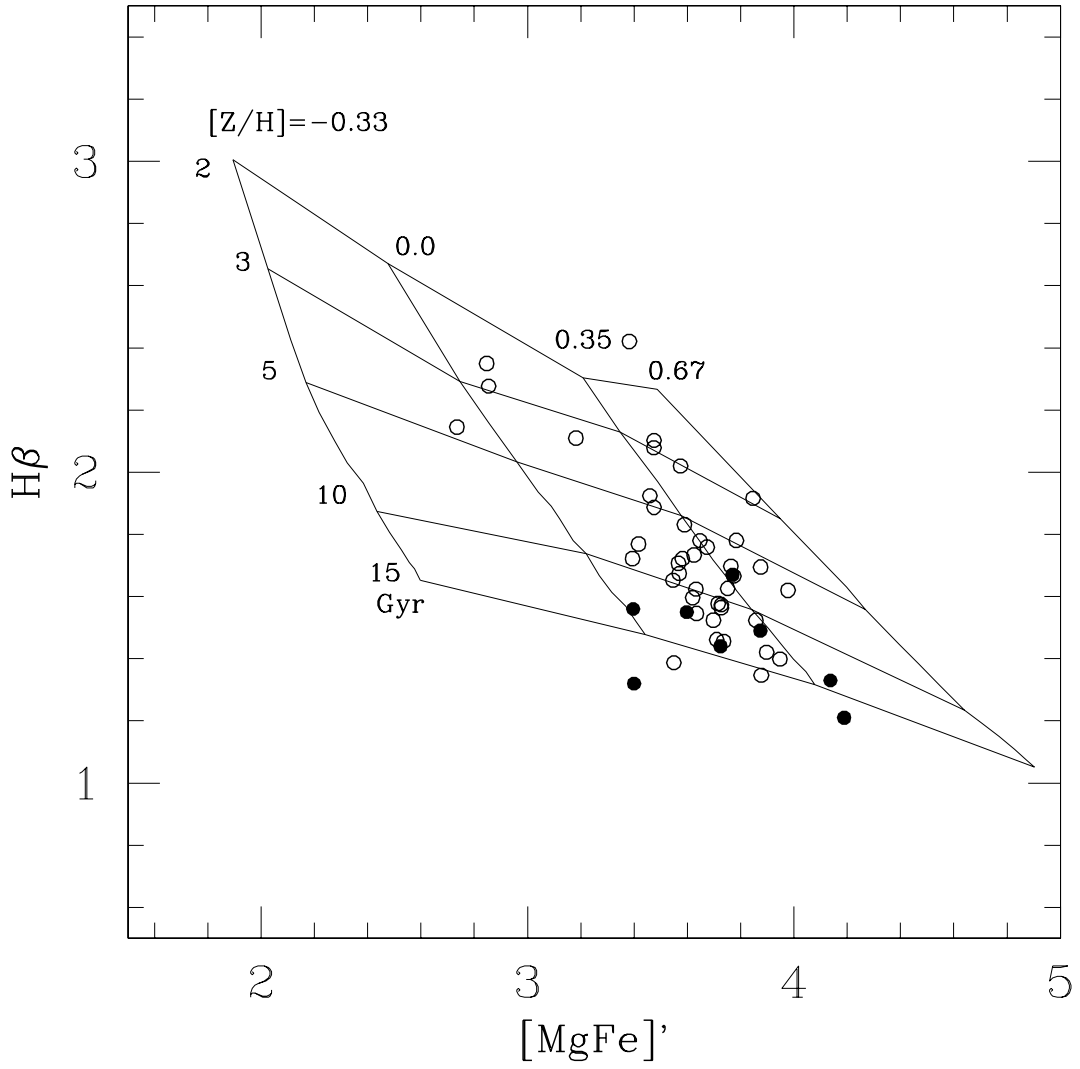

Fig. 6.— Compact group galaxies (filled circles), TMB03 models (grid) and field galaxies (open circles) in Hβ vs. [MgFe]' diagram. The index [MgFe]' follows TMB03 and is defined as [MgFe]' = (Mgb(0.72 Fe5270 + 0.28 Fe5335). Labels are given to illustrate the loci occupied by different stellar population parameters. In each model sequence, ages increase from top-left to bottom-right.

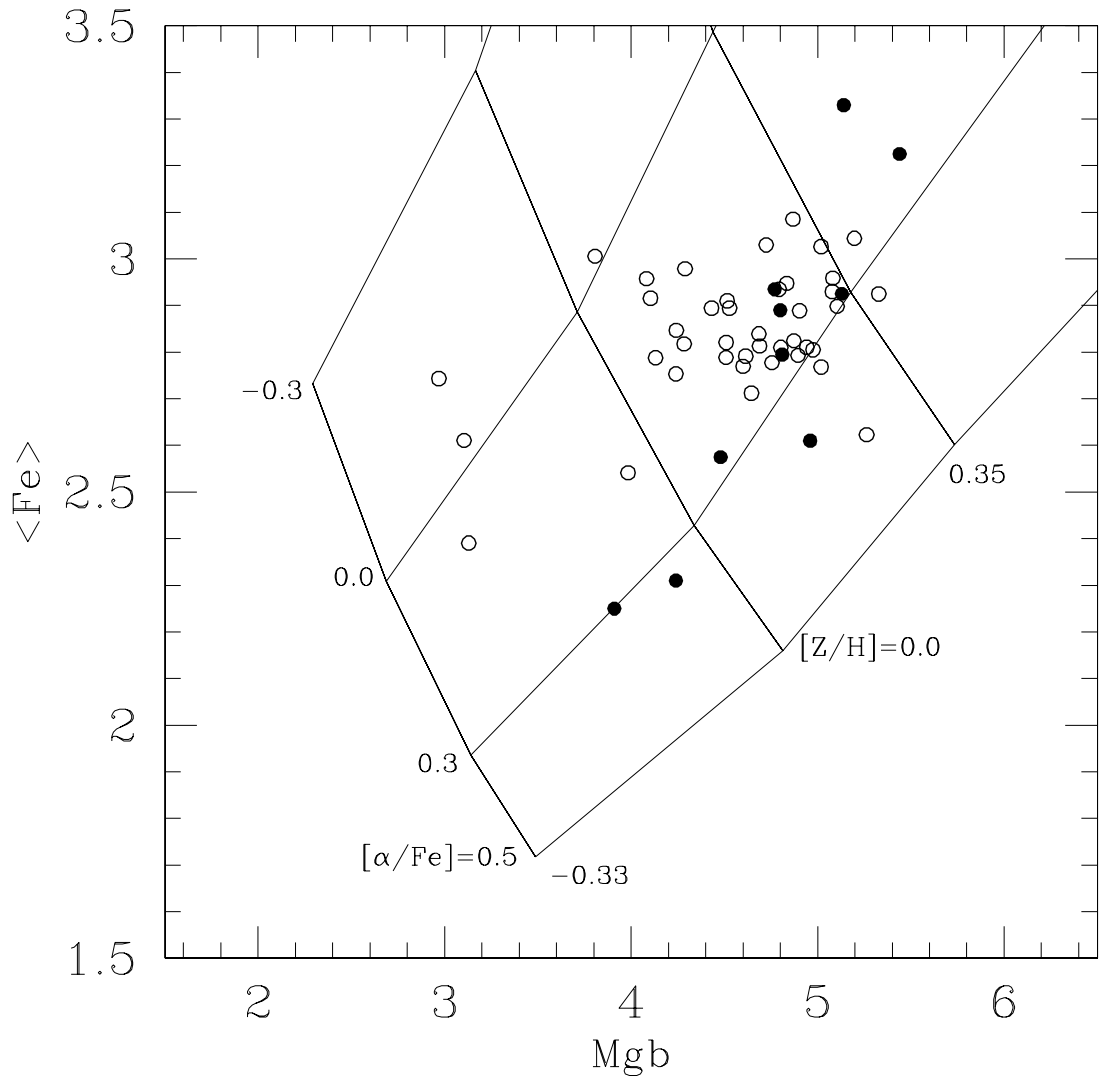

Fig. 7.— Compact group galaxies (filled circles), TMB03 models (grid) and field galaxies (open circles) in a Mg*b* vs. <Fe> diagram. Labels are given to illustrate the loci occupied by different stellar population parameters. The models are plotted for an age t = 12 Gyr.

Table 1. Main photometric and kinematic parameters for each galaxy

ID	r_{eff} in arcsec	μ_{eff} Type (Hickson)	S/N Type (NED)	V_{rad}	σ $km\ s^{-1}$	$\Delta\sigma$ $km\ s^{-1}$
04D*	4.0	20.22	30	8005.7	71.8	5.2
05B	7.0	21.21	49	11944.7	205.6	5.2
13B*	8.5	21.83	36	12114.2	196.1	5.8
14B*	64.0	24.06	38	5188.8	157.5	4.8
21C	21.0	22.83	77	7208.3	224.0	3.4
76B	10.0	21.47	36	9882.1	186.0	5.8
76C	12.0	22.07	45	10473.8	223.5	5.2
76D	6.0	21.52	30	10108.9	150.5	5.4
86A	15.7	21.33	70	5923.1	291.7	4.4
86B*	8.0	20.70	54	5805.2	215.0	3.7
90B	12.0	20.40	75	2502.0	235.6	3.2
90C	14.7	20.73	74	2550.9	198.0	2.9
93A*	22.0	21.78	54	4956.7	239.5	4.9
94A	11.7	21.91	39	11765.1	267.3	7.3
94B	11.9	21.86	42	11783.8	310.2	7.3
97A	40.2	23.27	23	6818.3	201.1	7.8

(*)Has emission lines

Table 2. Line indices for the compact group galaxies

ID	$H\beta$	Mg_1	Mg_2	Mg_b	Fe_{5015}	Fe_{5270}	Fe_{5335}	Fe_{5406}
04D	···	0.055±0.005	0.111±0.005	2.04±0.20	3.15±0.41	1.32±0.23	1.59±0.19	0.90±0.14
05B	1.67±0.23	0.156±0.004	0.318±0.005	4.54±0.19	4.94±0.40	3.36±0.19	2.90±0.20	1.83±0.15
13B	···	0.149±0.005	0.282±0.006	4.07±0.21	4.05±0.42	3.39±0.22	3.14±0.28	1.74±0.26
14B	···	0.083±0.004	0.207±0.004	3.91±0.16	4.08±0.34	2.39±0.17	2.11±0.16	1.37±0.12
21C	1.32±0.12	0.121±0.002	0.276±0.003	4.33±0.10	4.93±0.24	2.92±0.11	2.42±0.12	1.75±0.10
76B	1.23±0.29	0.133±0.005	0.284±0.006	4.24±0.22	5.64±0.45	2.58±0.22	2.04±0.27	1.57±0.22
76C	1.44±0.16	0.144±0.004	0.299±0.004	4.80±0.17	5.88±0.36	2.82±0.17	2.96±0.20	1.92±0.15
76D	1.55±0.22	0.124±0.005	0.280±0.006	4.96±0.22	3.81±0.53	2.61±0.23	1.32±0.23	1.32±0.27
86A	1.33±0.12	0.172±0.002	0.350±0.003	5.14±0.13	6.09±0.28	3.60±0.13	3.06±0.16	1.81±0.13
86B	···	0.136±0.003	0.299±0.004	4.77±0.14	4.79±0.30	2.95±0.15	2.92±0.16	1.69±0.13
90B	1.49±0.12	0.158±0.002	0.317±0.003	5.13±0.10	5.67±0.21	3.17±0.10	2.68±0.12	1.92±0.10
90C	1.56±0.11	0.131±0.002	0.287±0.003	4.48±0.10	4.88±0.22	2.81±0.10	2.34±0.11	1.84±0.08
93A	···	0.113±0.003	0.265±0.004	4.81±0.17	4.44±0.36	3.04±0.18	2.55±0.18	1.91±0.13
94A	1.21±0.22	0.159±0.005	0.320±0.007	5.44±0.25	5.28±0.59	3.54±0.26	2.91±0.33	1.67±0.26
94B	0.57±0.32	0.168±0.009	0.298±0.012	4.96±0.45	5.82±1.00	3.40±0.46	2.82±0.49	1.68±0.35
97A	1.92±0.43	0.124±0.008	0.280±0.010	4.70±0.40	4.74±0.79	3.28±0.40	2.68±0.49	2.01±0.29

Table 3. Fitting function coefficients for Mg_2 index.

	Validity	$5000 \leq T_{\rm eff} \leq 7000$	$5000 \leq T_{\rm eff} \leq 7000$	$4000 \leq T_{\rm eff} \leq 5000$(*)
	range	$0.0 \leq \log g \leq 5.0$	$0.0 \leq \log g \leq 5.0$	$0.0 < \log g \leq 5.0$
		$-3.0 \leq$ [Fe/H] ≤ -1.0	$-1.0 \leq$ [Fe/H] $\leq +0.3$	$-3.0 \leq$ [Fe/H] $\leq +0.3$
Coefficient	Term			
a	constant	-2.4823	-2.5161	0.0141
b	$\log \theta$	-2.7275	0.0104	-2.1352
c	$(\log \theta)^2$	0	22.2153	37.7958
d	$(\log \theta)^3$	0	0	0
e	$\log g$	-0.0218	-0.1128	-0.0616
f	$(\log g)^2$	0	0.0421	0.0185
g	$(\log g)^3$	0.01043	0.0088	0
h	[Fe/H]	0.41801	0.6361	0.0899
i	$[\mathrm{Fe/H}]^2$	-0.112	0	0
j	$[\mathrm{Fe/H}]^3$	0	0	0
k	$[\alpha/\mathrm{Fe}]$	0.8161	0.81051	0.0904
l	$(\log \theta)(\log g)$	4.5051	3.0778	2.4707
m	$(\log \theta)([\mathrm{Fe/H}])$	1.4022	1.4763	0.7067
n	$(\log \theta)([\alpha/\mathrm{Fe}])$	4.3325	3.8713	1.4655
o	$(\log \theta)^2(\log g)$	14.560	6.6195	-11.4960
p	$(\log \theta)(\log g)^2$	0.1697	0.2266	-0.2505
	r.m.s.	0.007	0.014	0.038

(*)This interval is not described in terms of exponential. The index is given directly by the polynomial form inside the parenthesis in the equation in the text.

Table 4. Fitting function coefficients for Fe5270 index.

Validity range		$4000 \leq T_{\rm eff} \leq 7000$ $0.0 \leq \log g \leq 3.0$ $-3.0 \leq$ [Fe/H] $\leq +0.3$	$4000 \leq T_{\rm eff} \leq 4750$ $3.0 \leq \log g \leq 5.0$ $-3.0 \leq$ [Fe/H] $\leq +0.3$	$4750 \leq T_{\rm eff} \leq 7000$ $3.0 < \log g \leq 5.0$ $-3.0 \leq$ [Fe/H] $\leq +0.3$
Coefficient	Term			
a	constant	1.6686	0.4078	1.4406
b	$\log \theta$	-0.6681	10.8621	-1.3135
c	$(\log \theta)^2$	7.2196	-18.6671	36.3395
d	$(\log \theta)^3$	56.9337	0	0
e	$\log g$	-0.2003	0.1996	-0.2830
f	$(\log g)^2$	0	0	0.0509
g	$(\log g)^3$	0	0	0
h	[Fe/H]	0.5467	0.5234	0.46607
i	$[\mathrm{Fe/H}]^2$	-0.0316	0	-0.0150
j	$[\mathrm{Fe/H}]^3$	0.0163	0.0284	0.0310
k	$[\alpha/\mathrm{Fe}]$	0.0493	-0.1458	-0.0755
l	$(\log \theta)(\log g)$	0.5784	-1.2399	1.9521
m	$(\log \theta)([\mathrm{Fe/H}])$	-1.7989	-2.7461	-2.6080
n	$(\log \theta)([\alpha/\mathrm{Fe}])$	0	-1.3704	-1.6855
o	$(\log \theta)^2(\log g)$	4.3268	0	-3.4429
p	$(\log \theta)(\log g)^2$	0.2522	0	0
	r.m.s.	0.20	0.22	0.07

Table 5. Fitting function coefficients for Fe5335 index.

Validity range		$4000 \leq T_{\rm eff} \leq 7000$ $0.0 \leq \log g \leq 3.0$ $-3.0 \leq$ [Fe/H] $\leq +0.3$	$4000 \leq T_{\rm eff} \leq 4750$ $3.0 \leq \log g \leq 5.0$ $-3.0 \leq$ [Fe/H] $\leq +0.3$	$4750 \leq T_{\rm eff} \leq 7000$ $3.0 < \log g \leq 5.0$ $-3.0 \leq$ [Fe/H] $\leq +0.3$
Coefficient	Term			
a	constant	1.5212	0.2631	1.2824
b	$\log \theta$	1.2643	13.5966	0
c	$(\log \theta)^2$	10.4707	-23.3170	38.6002
d	$(\log \theta)^3$	38.8133	0	0
e	$\log g$	-0.1578	0.24554	-0.2363
f	$(\log g)^2$	-0.0077	0	0.0492
g	$(\log g)^3$	0	0	0
h	[Fe/H]	0.5273	0.5849	0.4698
i	$[\mathrm{Fe/H}]^2$	0	-0.07951	-0.0202
j	$[\mathrm{Fe/H}]^3$	0.0304	0	0.0333
k	$[\alpha/\mathrm{Fe}]$	-0.009	-0.2454	-0.2101
l	$(\log \theta)(\log g)$	0.5137	-1.5053	1.9031
m	$(\log \theta)([\mathrm{Fe/H}])$	-1.2216	-2.6334	-2.4474
n	$(\log \theta)([\alpha/\mathrm{Fe}])$	0	-2.4218	-1.7837
o	$(\log \theta)^2(\log g)$	2.7040	0	-4.0214
p	$(\log \theta)(\log g)^2$	0.2346	0	0
	r.m.s.	0.25	0.21	0.09

Table 6. Zero-points constants to be applied to indices derived from the fitting functions in order to calibrate them to the Lick/IDS system.

Index	Zero-point	σ
Mg_2	0.018	0.035
Fe5270	-0.40	0.53
Fe5335	-0.66	0.53

Table 7. Parameters for the best SSP fits to the compact group galaxies.

	TMB SSP models			This work SSP models		
ID	Age	$[Z/H]$	$[\alpha/Fe]$	$[Z/H]$	$[Fe/H]$	$[\alpha/Fe]$
HCG 05B	6	0.40	0.15	0.38	0.09	0.4
HCG 21C	19	-0.03	0.21	-0.08	-0.34	0.3
HCG 76C	13	0.23	0.24	0.11	-0.13	0.3
HCG 76D	13	0.07	0.45	0.02	-0.35	0.4
HCG 86A	13	0.42	0.17	0.38	0.17	0.3
HCG 90B	11	0.36	0.30	0.25	-0.06	0.4
HCG 90C	12	0.07	0.28	0.08	-0.25	0.4
HCG 94A	17	0.39	0.25	0.20	-0.01	0.2

A. Single stellar population model indices

Single stellar population models described in Section 3.3.

Table A.1. SSP models indices for Mg_2, Fe5270 and Fe5335.

Age (Gyr)	Z	$[\alpha/Fe]$	$[Fe/H]$	Mg_2	Fe52	Fe53
4	0.008	0.0	-0.37	0.141	1.992	1.694
5	0.008	0.0	-0.37	0.149	2.060	1.777
6	0.008	0.0	-0.37	0.157	2.150	1.882
7	0.008	0.0	-0.37	0.165	2.218	1.961
8	0.008	0.0	-0.37	0.171	2.278	2.033
9	0.008	0.0	-0.37	0.178	2.338	2.102
10	0.008	0.0	-0.37	0.183	2.379	2.153
11	0.008	0.0	-0.37	0.188	2.428	2.208
12	0.008	0.0	-0.37	0.194	2.480	2.269
13	0.008	0.0	-0.37	0.198	2.519	2.313
14	0.008	0.0	-0.37	0.201	2.538	2.336
15	0.008	0.0	-0.37	0.206	2.579	2.385
16	0.008	0.0	-0.37	0.210	2.617	2.429
4	0.008	0.2	-0.51	0.151	1.861	1.527
5	0.008	0.2	-0.51	0.157	1.911	1.585
6	0.008	0.2	-0.51	0.166	1.988	1.671
7	0.008	0.2	-0.51	0.175	2.063	1.758
8	0.008	0.2	-0.51	0.181	2.110	1.812
9	0.008	0.2	-0.51	0.191	2.186	1.899
10	0.008	0.2	-0.51	0.194	2.208	1.925
11	0.008	0.2	-0.51	0.201	2.263	1.988
12	0.008	0.2	-0.51	0.206	2.308	2.038
13	0.008	0.2	-0.51	0.212	2.354	2.091
14	0.008	0.2	-0.51	0.217	2.393	2.136
15	0.008	0.2	-0.51	0.222	2.431	2.180
16	0.008	0.2	-0.51	0.231	2.501	2.262
4	0.008	0.4	-0.67	0.158	1.696	1.331
5	0.008	0.4	-0.67	0.164	1.732	1.371
6	0.008	0.4	-0.67	0.172	1.799	1.443
7	0.008	0.4	-0.67	0.183	1.872	1.526
8	0.008	0.4	-0.67	0.189	1.917	1.575
9	0.008	0.4	-0.67	0.199	1.990	1.657
10	0.008	0.4	-0.67	0.204	2.020	1.691

Table A.1—Continued

Age (Gyr)	Z	$[\alpha/Fe]$	$[Fe/H]$	Mg_2	Fe52	Fe53
11	0.008	0.4	-0.67	0.212	2.073	1.751
12	0.008	0.4	-0.67	0.218	2.118	1.800
13	0.008	0.4	-0.67	0.225	2.172	1.861
14	0.008	0.4	-0.67	0.233	2.225	1.921
15	0.008	0.4	-0.67	0.238	2.262	1.962
4	0.01	0.0	-0.27	0.155	2.167	1.881
5	0.01	0.0	-0.27	0.163	2.243	1.973
6	0.01	0.0	-0.27	0.172	2.325	2.071
7	0.01	0.0	-0.27	0.182	2.418	2.180
8	0.01	0.0	-0.27	0.185	2.432	2.200
9	0.01	0.0	-0.27	0.193	2.500	2.280
10	0.01	0.0	-0.27	0.200	2.566	2.359
11	0.01	0.0	-0.27	0.203	2.586	2.383
12	0.01	0.0	-0.27	0.210	2.645	2.450
13	0.01	0.0	-0.27	0.216	2.703	2.517
14	0.01	0.0	-0.27	0.222	2.748	2.571
15	0.01	0.0	-0.27	0.225	2.766	2.595
16	0.01	0.0	-0.27	0.229	2.802	2.637
4	0.01	0.2	-0.41	0.164	2.024	1.695
5	0.01	0.2	-0.41	0.172	2.094	1.777
6	0.01	0.2	-0.41	0.181	2.156	1.848
7	0.01	0.2	-0.41	0.192	2.246	1.951
8	0.01	0.2	-0.41	0.195	2.260	1.970
9	0.01	0.2	-0.41	0.203	2.322	2.041
10	0.01	0.2	-0.41	0.210	2.376	2.102
11	0.01	0.2	-0.41	0.214	2.407	2.140
12	0.01	0.2	-0.41	0.222	2.468	2.210
13	0.01	0.2	-0.41	0.229	2.522	2.270
14	0.01	0.2	-0.41	0.236	2.576	2.334
15	0.01	0.2	-0.41	0.237	2.574	2.330
16	0.01	0.2	-0.41	0.246	2.645	2.414
4	0.01	0.4	-0.57	0.171	1.850	1.485
5	0.01	0.4	-0.57	0.181	1.922	1.567

Table A.1—Continued

Age (Gyr)	Z	$[\alpha/Fe]$	$[Fe/H]$	Mg_2	Fe52	Fe53
6	0.01	0.4	-0.57	0.187	1.962	1.610
7	0.01	0.4	-0.57	0.200	2.048	1.707
8	0.01	0.4	-0.57	0.203	2.064	1.725
9	0.01	0.4	-0.57	0.212	2.129	1.798
10	0.01	0.4	-0.57	0.220	2.183	1.858
11	0.01	0.4	-0.57	0.226	2.219	1.900
12	0.01	0.4	-0.57	0.234	2.278	1.967
13	0.01	0.4	-0.57	0.241	2.327	2.021
14	0.01	0.4	-0.57	0.250	2.397	2.102
15	0.01	0.4	-0.57	0.252	2.402	2.105
16	0.01	0.4	-0.57	0.262	2.475	2.190
4	0.014	0.0	-0.12	0.175	2.441	2.174
5	0.014	0.0	-0.12	0.185	2.525	2.277
6	0.014	0.0	-0.12	0.193	2.593	2.358
7	0.014	0.0	-0.12	0.203	2.670	2.453
8	0.014	0.0	-0.12	0.206	2.692	2.482
9	0.014	0.0	-0.12	0.214	2.754	2.559
10	0.014	0.0	-0.12	0.222	2.826	2.646
11	0.014	0.0	-0.12	0.228	2.860	2.685
12	0.014	0.0	-0.12	0.235	2.928	2.768
13	0.014	0.0	-0.12	0.242	2.979	2.827
14	0.014	0.0	-0.12	0.249	3.038	2.899
15	0.014	0.0	-0.12	0.253	3.059	2.928
16	0.014	0.0	-0.12	0.259	3.103	2.980
4	0.014	0.2	-0.26	0.182	2.265	1.944
5	0.014	0.2	-0.26	0.192	2.341	2.034
6	0.014	0.2	-0.26	0.201	2.399	2.101
7	0.014	0.2	-0.26	0.210	2.466	2.179
8	0.014	0.2	-0.26	0.215	2.492	2.213
9	0.014	0.2	-0.26	0.221	2.537	2.264
10	0.014	0.2	-0.26	0.231	2.614	2.353
11	0.014	0.2	-0.26	0.237	2.652	2.399
12	0.014	0.2	-0.26	0.246	2.721	2.480

Table A.1—Continued

Age (Gyr)	Z	$[\alpha/Fe]$	$[Fe/H]$	Mg_2	Fe52	Fe53
13	0.014	0.2	-0.26	0.253	2.768	2.536
14	0.014	0.2	-0.26	0.260	2.819	2.594
15	0.014	0.2	-0.26	0.262	2.826	2.598
4	0.014	0.4	-0.42	0.189	2.080	1.716
5	0.014	0.4	-0.42	0.201	2.161	1.809
6	0.014	0.4	-0.42	0.209	2.199	1.849
7	0.014	0.4	-0.42	0.219	2.260	1.919
8	0.014	0.4	-0.42	0.224	2.291	1.956
9	0.014	0.4	-0.42	0.231	2.333	2.003
10	0.014	0.4	-0.42	0.241	2.410	2.090
11	0.014	0.4	-0.42	0.248	2.449	2.133
12	0.014	0.4	-0.42	0.258	2.518	2.214
13	0.014	0.4	-0.42	0.265	2.559	2.260
14	0.014	0.4	-0.42	0.273	2.619	2.328
15	0.014	0.4	-0.42	0.275	2.618	2.325
16	0.014	0.4	-0.42	0.284	2.681	2.397
4	0.018	0.0	0.00	0.188	2.632	2.379
5	0.018	0.0	0.00	0.200	2.732	2.502
6	0.018	0.0	0.00	0.209	2.797	2.579
7	0.018	0.0	0.00	0.216	2.847	2.644
8	0.018	0.0	0.00	0.224	2.911	2.723
9	0.018	0.0	0.00	0.230	2.955	2.782
10	0.018	0.0	0.00	0.239	3.026	2.867
11	0.018	0.0	0.00	0.247	3.087	2.945
12	0.018	0.0	0.00	0.256	3.151	3.023
13	0.018	0.0	0.00	0.261	3.190	3.070
14	0.018	0.0	0.00	0.269	3.251	3.146
15	0.018	0.0	0.00	0.276	3.295	3.201
16	0.018	0.0	0.00	0.282	3.347	3.269
4	0.018	0.2	-0.14	0.195	2.442	2.126
5	0.018	0.2	-0.14	0.206	2.522	2.222
6	0.018	0.2	-0.14	0.216	2.583	2.292
7	0.018	0.2	-0.14	0.223	2.623	2.342

Table A.1—Continued

Age (Gyr)	Z	$[\alpha/Fe]$	$[Fe/H]$	Mg_2	Fe52	Fe53
8	0.018	0.2	-0.14	0.231	2.683	2.413
9	0.018	0.2	-0.14	0.238	2.718	2.457
10	0.018	0.2	-0.14	0.248	2.800	2.552
11	0.018	0.2	-0.14	0.258	2.861	2.626
12	0.018	0.2	-0.14	0.266	2.928	2.705
13	0.018	0.2	-0.14	0.273	2.967	2.752
14	0.018	0.2	-0.14	0.279	3.010	2.805
15	0.018	0.2	-0.14	0.285	3.043	2.841
16	0.018	0.2	-0.14	0.293	3.096	2.905
4	0.018	0.4	-0.30	0.203	2.249	1.885
5	0.018	0.4	-0.30	0.215	2.328	1.977
6	0.018	0.4	-0.30	0.224	2.376	2.029
7	0.018	0.4	-0.30	0.231	2.412	2.071
8	0.018	0.4	-0.30	0.241	2.470	2.138
9	0.018	0.4	-0.30	0.247	2.502	2.174
10	0.018	0.4	-0.30	0.260	2.587	2.273
11	0.018	0.4	-0.30	0.268	2.640	2.333
12	0.018	0.4	-0.30	0.279	2.712	2.416
13	0.018	0.4	-0.30	0.285	2.749	2.460
14	0.018	0.4	-0.30	0.293	2.793	2.508
15	0.018	0.4	-0.30	0.296	2.810	2.527
16	0.018	0.4	-0.30	0.305	2.862	2.587
4	0.022	0.0	0.09	0.198	2.785	2.540
5	0.022	0.0	0.09	0.213	2.912	2.699
6	0.022	0.0	0.09	0.222	2.974	2.776
7	0.022	0.0	0.09	0.229	3.017	2.833
8	0.022	0.0	0.09	0.240	3.101	2.940
9	0.022	0.0	0.09	0.246	3.143	2.993
10	0.022	0.0	0.09	0.256	3.209	3.078
11	0.022	0.0	0.09	0.265	3.282	3.169
12	0.022	0.0	0.09	0.274	3.346	3.248
13	0.022	0.0	0.09	0.280	3.386	3.301
14	0.022	0.0	0.09	0.287	3.441	3.368

Table A.1—Continued

Age (Gyr)	Z	$[\alpha/Fe]$	$[Fe/H]$	Mg_2	Fe52	Fe53
15	0.022	0.0	0.09	0.295	3.501	3.448
16	0.022	0.0	0.09	0.302	3.552	3.509
4	0.022	0.2	-0.05	0.206	2.585	2.272
5	0.022	0.2	-0.05	0.219	2.683	2.391
6	0.022	0.2	-0.05	0.229	2.744	2.463
7	0.022	0.2	-0.05	0.235	2.774	2.502
8	0.022	0.2	-0.05	0.246	2.850	2.593
9	0.022	0.2	-0.05	0.253	2.889	2.641
10	0.022	0.2	-0.05	0.264	2.964	2.733
11	0.022	0.2	-0.05	0.274	3.039	2.822
12	0.022	0.2	-0.05	0.284	3.102	2.897
13	0.022	0.2	-0.05	0.290	3.140	2.947
14	0.022	0.2	-0.05	0.297	3.180	2.991
15	0.022	0.2	-0.05	0.305	3.232	3.056
4	0.022	0.4	-0.21	0.213	2.379	2.012
5	0.022	0.4	-0.21	0.227	2.471	2.121
6	0.022	0.4	-0.21	0.237	2.526	2.183
7	0.022	0.4	-0.21	0.244	2.551	2.213
8	0.022	0.4	-0.21	0.255	2.618	2.290
9	0.022	0.4	-0.21	0.261	2.653	2.332
10	0.022	0.4	-0.21	0.274	2.733	2.424
11	0.022	0.4	-0.21	0.284	2.798	2.499
12	0.022	0.4	-0.21	0.295	2.862	2.574
13	0.022	0.4	-0.21	0.303	2.901	2.622
14	0.022	0.4	-0.21	0.309	2.937	2.662
15	0.022	0.4	-0.21	0.316	2.978	2.707
16	0.022	0.4	-0.21	0.323	3.017	2.755
4	0.026	0.0	0.17	0.207	2.929	2.694
5	0.026	0.0	0.17	0.226	3.080	2.885
6	0.026	0.0	0.17	0.235	3.138	2.962
7	0.026	0.0	0.17	0.244	3.195	3.036
8	0.026	0.0	0.17	0.253	3.268	3.133
9	0.026	0.0	0.17	0.263	3.328	3.202

Table A.1—Continued

Age (Gyr)	Z	$[\alpha/Fe]$	$[Fe/H]$	Mg_2	Fe52	Fe53
10	0.026	0.0	0.17	0.271	3.387	3.282
11	0.026	0.0	0.17	0.282	3.462	3.375
12	0.026	0.0	0.17	0.290	3.530	3.466
13	0.026	0.0	0.17	0.298	3.577	3.525
14	0.026	0.0	0.17	0.305	3.626	3.588
15	0.026	0.0	0.17	0.313	3.683	3.658
16	0.026	0.0	0.17	0.320	3.736	3.725
4	0.026	0.2	0.03	0.214	2.711	2.400
5	0.026	0.2	0.03	0.231	2.832	2.549
6	0.026	0.2	0.03	0.241	2.887	2.619
7	0.026	0.2	0.03	0.248	2.924	2.668
8	0.026	0.2	0.03	0.259	2.997	2.752
9	0.026	0.2	0.03	0.269	3.050	2.820
10	0.026	0.2	0.03	0.278	3.114	2.897
11	0.026	0.2	0.03	0.290	3.191	2.995
12	0.026	0.2	0.03	0.299	3.251	3.063
13	0.026	0.2	0.03	0.307	3.296	3.118
14	0.026	0.2	0.03	0.313	3.332	3.167
15	0.026	0.2	0.03	0.322	3.391	3.239
16	0.026	0.2	0.03	0.328	3.432	3.288
4	0.026	0.4	-0.13	0.220	2.488	2.120
5	0.026	0.4	-0.13	0.239	2.603	2.256
6	0.026	0.4	-0.13	0.249	2.660	2.322
7	0.026	0.4	-0.13	0.256	2.685	2.351
8	0.026	0.4	-0.13	0.266	2.746	2.422
9	0.026	0.4	-0.13	0.276	2.797	2.484
10	0.026	0.4	-0.13	0.286	2.858	2.557
11	0.026	0.4	-0.13	0.298	2.927	2.635
12	0.026	0.4	-0.13	0.307	2.983	2.703
13	0.026	0.4	-0.13	0.316	3.026	2.754
14	0.026	0.4	-0.13	0.324	3.063	2.799
15	0.026	0.4	-0.13	0.332	3.118	2.864
16	0.026	0.4	-0.13	0.339	3.151	2.899

Table A.1—Continued

Age (Gyr)	Z	$[\alpha/Fe]$	$[Fe/H]$	Mg_2	Fe52	Fe53
4	0.03	0.0	0.24	0.216	3.064	2.842
5	0.03	0.0	0.24	0.238	3.232	3.054
6	0.03	0.0	0.24	0.246	3.283	3.125
7	0.03	0.0	0.24	0.257	3.354	3.217
8	0.03	0.0	0.24	0.266	3.419	3.304
9	0.03	0.0	0.24	0.278	3.500	3.405
10	0.03	0.0	0.24	0.286	3.549	3.468
11	0.03	0.0	0.24	0.297	3.627	3.567
12	0.03	0.0	0.24	0.306	3.694	3.653
13	0.03	0.0	0.24	0.315	3.749	3.722
14	0.03	0.0	0.24	0.321	3.792	3.783
15	0.03	0.0	0.24	0.330	3.849	3.854
16	0.03	0.0	0.24	0.337	3.906	3.934
4	0.03	0.2	0.10	0.221	2.823	2.516
5	0.03	0.2	0.10	0.242	2.963	2.687
6	0.03	0.2	0.10	0.252	3.013	2.754
7	0.03	0.2	0.10	0.260	3.057	2.810
8	0.03	0.2	0.10	0.271	3.128	2.898
9	0.03	0.2	0.10	0.281	3.193	2.975
10	0.03	0.2	0.10	0.291	3.248	3.043
11	0.03	0.2	0.10	0.302	3.325	3.141
12	0.03	0.2	0.10	0.313	3.384	3.212
13	0.03	0.2	0.10	0.320	3.435	3.280
14	0.03	0.2	0.10	0.328	3.467	3.321
15	0.03	0.2	0.10	0.336	3.531	3.400
4	0.03	0.4	-0.06	0.228	2.590	2.220
5	0.03	0.4	-0.06	0.249	2.720	2.374
6	0.03	0.4	-0.06	0.260	2.774	2.440
7	0.03	0.4	-0.06	0.267	2.800	2.474
8	0.03	0.4	-0.06	0.278	2.863	2.543
9	0.03	0.4	-0.06	0.288	2.923	2.617
10	0.03	0.4	-0.06	0.298	2.971	2.676
11	0.03	0.4	-0.06	0.311	3.039	2.758

Table A.1—Continued

Age (Gyr)	Z	$[\alpha/Fe]$	$[Fe/H]$	Mg_2	Fe52	Fe53
12	0.03	0.4	-0.06	0.319	3.092	2.819
13	0.03	0.4	-0.06	0.329	3.140	2.880
14	0.03	0.4	-0.06	0.336	3.177	2.922
15	0.03	0.4	-0.06	0.347	3.241	2.998
16	0.03	0.4	-0.06	0.352	3.274	3.037
4	0.035	0.0	0.32	0.226	3.223	3.012
5	0.035	0.0	0.32	0.250	3.398	3.236
6	0.035	0.0	0.32	0.259	3.447	3.311
7	0.035	0.0	0.32	0.272	3.537	3.431
8	0.035	0.0	0.32	0.280	3.592	3.506
9	0.035	0.0	0.32	0.294	3.686	3.615
10	0.035	0.0	0.32	0.303	3.736	3.683
11	0.035	0.0	0.32	0.313	3.810	3.778
12	0.035	0.0	0.32	0.324	3.880	3.869
13	0.035	0.0	0.32	0.333	3.945	3.956
14	0.035	0.0	0.32	0.340	3.979	4.003
15	0.035	0.0	0.32	0.348	4.040	4.082
16	0.035	0.0	0.32	0.357	4.094	4.151
4	0.035	0.2	0.18	0.230	2.956	2.655
5	0.035	0.2	0.18	0.254	3.107	2.841
6	0.035	0.2	0.18	0.263	3.155	2.906
7	0.035	0.2	0.18	0.272	3.206	2.972
8	0.035	0.2	0.18	0.283	3.275	3.058
9	0.035	0.2	0.18	0.296	3.350	3.148
10	0.035	0.2	0.18	0.305	3.399	3.214
11	0.035	0.2	0.18	0.317	3.475	3.307
12	0.035	0.2	0.18	0.327	3.535	3.385
13	0.035	0.2	0.18	0.337	3.591	3.455
14	0.035	0.2	0.18	0.342	3.621	3.495
15	0.035	0.2	0.18	0.353	3.688	3.585
16	0.035	0.2	0.18	0.359	3.730	3.630
4	0.035	0.4	0.02	0.237	2.705	2.333
5	0.035	0.4	0.02	0.259	2.845	2.502

Table A.1—Continued

Age (Gyr)	Z	$[\alpha/Fe]$	$[Fe/H]$	Mg_2	Fe52	Fe53
6	0.035	0.4	0.02	0.270	2.898	2.569
7	0.035	0.4	0.02	0.278	2.928	2.606
8	0.035	0.4	0.02	0.291	2.993	2.680
9	0.035	0.4	0.02	0.303	3.060	2.762
10	0.035	0.4	0.02	0.312	3.097	2.811
11	0.035	0.4	0.02	0.323	3.164	2.891
12	0.035	0.4	0.02	0.334	3.216	2.950
13	0.035	0.4	0.02	0.342	3.271	3.019
14	0.035	0.4	0.02	0.352	3.310	3.063
15	0.035	0.4	0.02	0.361	3.376	3.149
4	0.04	0.0	0.39	0.236	3.372	3.175
5	0.04	0.0	0.39	0.261	3.542	3.398
6	0.04	0.0	0.39	0.271	3.594	3.477
7	0.04	0.0	0.39	0.286	3.694	3.608
8	0.04	0.0	0.39	0.294	3.746	3.681
9	0.04	0.0	0.39	0.309	3.847	3.796
10	0.04	0.0	0.39	0.317	3.898	3.870
11	0.04	0.0	0.39	0.329	3.973	3.966
12	0.04	0.0	0.39	0.339	4.048	4.068
13	0.04	0.0	0.39	0.350	4.113	4.152
14	0.04	0.0	0.39	0.355	4.149	4.203
15	0.04	0.0	0.39	0.365	4.207	4.278
16	0.04	0.0	0.39	0.372	4.259	4.344
4	0.04	0.2	0.25	0.239	3.080	2.786
5	0.04	0.2	0.25	0.263	3.232	2.974
6	0.04	0.2	0.25	0.274	3.284	3.048
7	0.04	0.2	0.25	0.284	3.340	3.121
8	0.04	0.2	0.25	0.295	3.404	3.199
9	0.04	0.2	0.25	0.310	3.486	3.301
10	0.04	0.2	0.25	0.318	3.533	3.362
11	0.04	0.2	0.25	0.331	3.610	3.463
12	0.04	0.2	0.25	0.341	3.669	3.535
13	0.04	0.2	0.25	0.352	3.729	3.611

Table A.1—Continued

Age (Gyr)	Z	$[\alpha/Fe]$	$[Fe/H]$	Mg_2	Fe52	Fe53
14	0.04	0.2	0.25	0.358	3.762	3.661
15	0.04	0.2	0.25	0.369	3.828	3.738
16	0.04	0.2	0.25	0.375	3.875	3.803
4	0.04	0.4	0.09	0.245	2.813	2.442
5	0.04	0.4	0.09	0.268	2.955	2.614
6	0.04	0.4	0.09	0.280	3.010	2.685
7	0.04	0.4	0.09	0.289	3.044	2.727
8	0.04	0.4	0.09	0.301	3.108	2.801
9	0.04	0.4	0.09	0.315	3.179	2.891
10	0.04	0.4	0.09	0.323	3.213	2.934
11	0.04	0.4	0.09	0.336	3.280	3.014
12	0.04	0.4	0.09	0.344	3.330	3.077
13	0.04	0.4	0.09	0.356	3.390	3.146
14	0.04	0.4	0.09	0.363	3.431	3.200
15	0.04	0.4	0.09	0.375	3.497	3.282

REFERENCES

Athanassoula, E., Makino, J. & Bosma, A., 1997, MNRAS, 286, 825

Barbuy, B., Perrin, M.-N., Katz, D., Coelho, P., Cayrel, R., Spite, M., van't Veer Menneret, C. 2003, A&A, 404, 661

Barnes, J.E., Hernquist, L. 1992, ARA&A, 30, 705

Bernardi, M., Renzini, A., da Costa, L. 1998, ApJ, 508, L143

Burstein, D., Davies, R.L., Dressler, A., Faber, S.M., Stone, R.S., Lynden-Bell, D., Terlevich, R. 1987, ApJS, 64, 601

Burstein, D., Faber, S. M., Gaskell, C. M., Krumm, N. 1984, ApJ 287, 586

de Vaucouleurs, G. 1948, Annales d'Astrophysique, 11, 247

Demarque, Woo, Kim, & Yi 2004, ApJS, in press

Diaferio, A., Geller, M.J., Ramella, M. 1994, AJ, 107, 868

Faber, S.M., Friel, E.D., Burstein, D., Gaskell, C.M. 1985, ApJS, 57, 711

González, J.J. 1993, PhD thesis, Lick Observatory, University of Santa Cruz

Governato, F., Tozzi, P., Cavaliere, A. 1996, ApJ, 458, 18

Greggio, L. 1997, MNRAS 285, 151

Hickson, P. 1982, ApJ, 255, 382

Hickson, P., Kindl, E., Huchra, J. 1988, ApJ, 331, 64

Jorgensen, I. 1997, MNRAS 288, 161

Jorgensen et al. 1995, MNRAS 276, 1341

Jorgensen, I. 1999, MNRAS, 306, 607

Maraston, C. 1998, MNRAS, 300, 872

Maraston, C. 2005, MNRAS, accepted.

Maraston, C., Thomas, D. 2000, ApJ 541, 126

Mendes de Oliveira, C. 1992, Ph.D. Thesis, U. of British Columbia, Canada

Mendes de Oliveira, C. 1993, Cosmic Velocity Fields, Ed. Bouchet, F.R., Lachièze-Rey, M. Gif-sur-Yvette: Ed. Frontieres, p. 563.

Moles, M., del Olmo, A., Perea, J., Masegosa, J., Marquez, I., Costa, V. 1994, A&A, 285, 404

Peletier, R. 1989, Ph.D. Thesis, University of Groningen, The Netherlands

Peletier 1999, *in The Evolution of Galaxies on Cosmological Timescales*, ASP Conf Series 187, p. 231

Phillips, M. M., Jenkins, C. R., Dopita, M. A., Sadler, E. M., Binette, L. 1986, AJ 91, 106

Plez, B., Brett, J.M., Nordlund, Å. 1992, A&A 256, 551

Proctor, R., Forbes, D., Hau, G., Beasley, M., De Silva, G. M., Contreras, R., Terlevich, A. I. 2004, MNRAS 349, 1381

Renzini, A., Buzzoni, 1986, in *Spectral Evolution of Galaxies*, eds. C. Chiosi, A. Renzini,

Rose, J., Bower, R.G., Caldwell, N. et al. 1994, AJ, 108, 2054

Rubin, V. C., Hunter, D. A., Ford, W. K. Jr. 1991, ApJS 76, 153

Salaris, M., Chieffi, A., Straniero, O. 1993, ApJ 414, 580

Salaris, M.; Weiss, A., 1998 A&A 335, 943

Salasnich, B.; Girardi, L.; Weiss, A.; Chiosi, C., 2000 A&A 361, 1023

Straniero, O.; Chieffi, A.; Salaris, M. 1992, Societa Astronomica Italiana 63, 43

Thomas, D., Maraston, C., Bender, R. 2003, MNRAS, 339, 897, TMB03

Thomas, D., Maraston, C., Bender, Mendes de Oliveira, 2005, in press.

Trager, S. C., Worthey, G., Faber, S. M., Burstein, D., Gonzalez, J. 1998, ApJS 116, 1

Tripicco, M.J., Bell, R.A. 1995, AJ,110, 3035

Vazdekis, A. 1999, ApJ 513, 224

Worthey, G., Faber, S.M., González, J.J. 1992, ApJ, 398, 69

Worthey, G., Faber, S.M., González, J.J., Burstein, D. 1994, ApJS, 94, 687

Worthey, G. 1998, PASP 110, 888

Zabludoff, A., Mulchaey, J. 1998, ApJ 496, 39

Zepf, S.E., Whitmore,B.C. 1991a, ApJ, 383, 542

Zepf, S.E., Whitmore, B.C., Levison, H.F. 1991b, ApJ, 383, 524

Zepf, S.E., Whitmore,B.C. 1993, ApJ, 418, 72

This preprint was prepared with the AAS LaTeX macros v5.2.